

Control mechanism for the upper airway collapse in patients with obstructive sleep apnea syndrome: a finite element study

HUANG RenHan¹, LI XiPing² & RONG QiGuo^{1*}

¹College of Engineering, Peking University, Beijing 100871, China;

²Department of Otolaryngology, Beijing Anzhen Hospital, Capital Medical University, Beijing 100029, China

Received September 28, 2012; accepted January 10, 2013; published online March 12, 2013

Obstructive sleep apnea syndrome (OSAS) is characterized by recurrent collapses of the upper airway, which lead to repetitive transient hypoxia, arousals and finally sleep fragmentation. Both anatomical and neuromuscular factors may play key roles in the pathophysiology of OSAS. The purpose of this paper was to study the control mechanism of OSAS from the mechanical point of view. A three-dimensional finite element model was developed, which not only reconstructed the realistic anatomical structure of the human upper airway, but also included surrounding structures such as the skull, neck, hyoid, cartilage and soft tissues. The respiration process during the normal and apnea states was simulated with the fluid-structure interaction method (FSI) and the computational fluid dynamics method (CFD). The airflow and deformation of the upper airway obtained from the FSI and the CFD method were compared and the results obtained under large negative pressure during an apnea episode were analyzed. The simulation results show that the FSI method is more feasible and effective than the CFD method. The concave configuration of the upper airway may accelerate the collapse of the upper airway in a positive feedback mechanism, which supplies meaningful information for clinical treatment and further research of OSAS.

upper airway collapse, sleep apnea, FEM, fluid-structure interaction

Citation: Huang R H, Li X P, Rong Q G. Control mechanism for the upper airway collapse in patients with obstructive sleep apnea syndrome: a finite element study. *Sci China Life Sci*, 2013, 56: 366–372, doi: 10.1007/s11427-013-4448-6

Obstructive sleep apnea syndrome (OSAS) is a common sleep-related breathing disorder characterized by repetitive pharyngeal collapse, cessation and reopening of the airflow in the oral and nasal cavity. Two factors may play key roles in the pathophysiology of OSAS: anatomic abnormalities of the upper airway and the weakness or absence of nerve control. Upper airway narrowing is often observed in OSAS patients. To obtain enough airflow during inspiration, more negative pressure is needed at the narrow part of the upper airway. In return, the negative pressure causes further narrowing and eventually the collapse. In addition, required by the needs of speech, swallowing, respiration and other physiological function, a complex nerve control system with

more than twenty various muscles plays a role in the upper airway. These groups of muscles interact in a complex fashion, undergoing contraction or relaxation according to the breath state. If the nerve control becomes weak or even absent, the upper airway may collapse under a normal small negative pressure [1–5].

From a mechanical point of view, the airflow in the upper airway is a process with fluid and structural interactions. The surrounding soft tissues possess not only nonlinear mechanical properties but also the abilities of self-adaptation [6–8]. Many mechanical models have been developed in the last few years to study the motion state of the upper airway during apnea. The aim of these studies was to find the critical conditions under which the upper airway loses its structural stability and begins to collapse.

*Corresponding author (email: qrong@pku.edu.cn)

Currently, the biomechanical models of OSAS can be classified into two main types: namely the lumped parameter models [9–11] and distributed parameter models. The distributed parameter model, usually a finite element model, has recently become popular because the distribution of meaningful quantities such as velocity, pressure, deformation and strain can be obtained. Some studies focus on the computational fluid dynamics simulations of respiration in order to investigate the fluid flow inside the airway regions where obstruction could occur. Geometrical models with anatomic details have been adopted in these studies and various computational fluid approaches have been used such as the unsteady large eddy model, steady Reynolds-Averaged Navier-Stokes with two-equation turbulence model and one-equation Spalart-Allmaras model. The restriction of these studies lies in that the influence of deformation of the airway wall is not taken into account [12–18]. Although some studies have paid attention to the interaction effect between airflow and soft tissue deformation, the geometrical model was usually oversimplified due to anatomical complexity and the huge cost of the coupled algorithm [19–23].

In this paper, a finite element model was established with more realistic anatomical details, such as the airway, skull, neck, hyoid and soft tissues around the upper airway. Respiration processes under normal and apnea conditions were

simulated in view of the fluid structure interaction.

1 Method

A set of CT image data obtained from a 26-year-old male was used for FE modeling. The CT data were first processed by a medical image processing software (Mimics 10.0, Belgium) and different anatomic structures, such as the skull, neck, hyoid, airway and the surrounding soft tissues were reconstructed. The results of Mimics are points cloud for each structure, and these were then exported to an inverse CAD software (Geomagic Studio 10.0, USA), in which some geometric singularities were corrected artificially and finally a 3D model with NURB surfaces was established. The geometric model was then imported into the FE software for meshing.

In speech, swallowing, respiration and other physiological functions, a number of intricate cartilage structures interact as a system around the epiglottis and hypopharynx, which prevent the upper airway wall from excessive expansion or contraction. In this study, the surrounding cartilages were taken into account and were modeled with shell elements. The whole FE model is shown in Figure 1. The information of the FE model is given in Table 1.

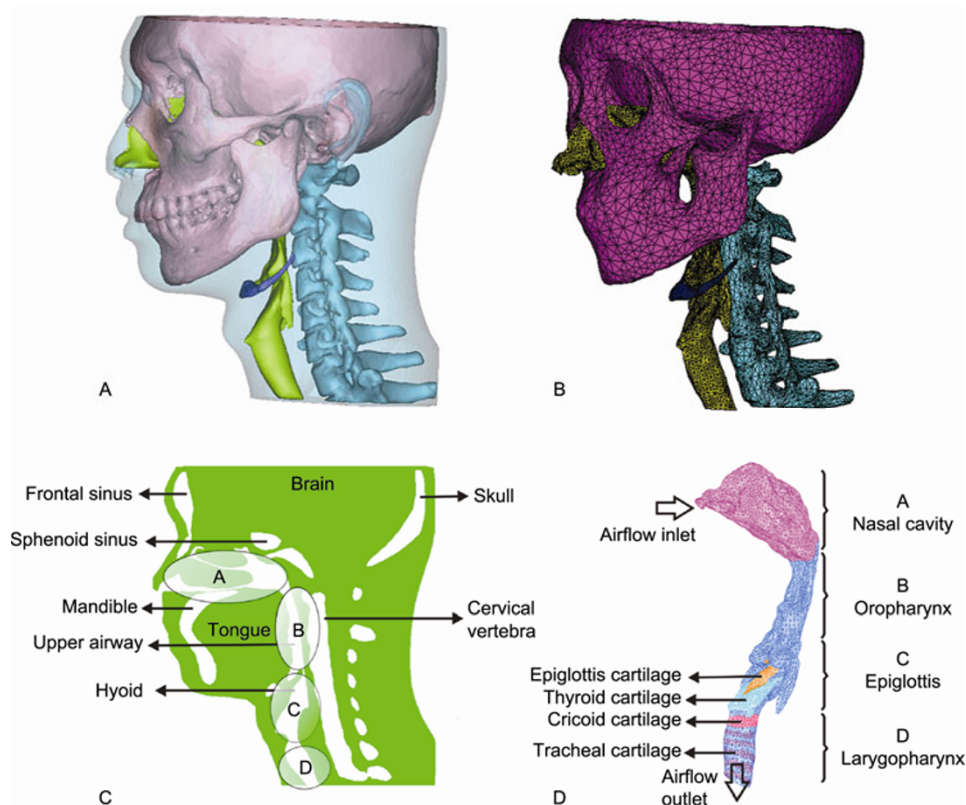


Figure 1 Three-dimensional upper airway model based on reconstructed CT data. A, Segmentation results including skull, neck, hyoid, upper airway and soft tissue. B, FE mesh of the bone tissue. C, The sagittal section of the model. Four ellipses indicated different parts possessing different material properties. D, The upper airway with a layer of shell element meshed on the lumen wall. A zero pressure is applied at the nostril while a time dependent pressure is exerted on the outlet surface.

For the sake of simplicity, linear constitutive relations were used for all tissues. Since water is the major component of the soft tissue, it could be considered as a quasi-incompressible material and so has a high Poisson ratio. The detailed material property for different tissues is given in Table 2. For the air flow simulation, a viscous incompressible laminar transient flow model was chosen. The density of airflow was $1.297 \times 10^{-6} \text{ g mm}^{-3}$ and the viscosity coefficient was $1.81 \times 10^{-5} \text{ Pa}$.

In the study, the dynamic pressure in the laryngeal part was applied as the load condition, which was acquired clinically by catheter manometer [24]. Two typical sets of pressure data, lasting about 12 s during normal breath and an apnea episode respectively, were extracted from the pressure data curve measured at the hypopharynx part and were applied as the distributed pressure on the outlet surface of the lumen, as is shown in Figure 2. At the nostril or airflow inlet, a zero pressure is applied instead of the atmospheric pressure since the pressure value used in the outlet has been already subtracted by the atmospheric pressure according to the titration principle used in the measurement.

The fluid-structure coupled simulation of respiratory

Table 1 Node and element information for FEM model

	Skull solid	Neck solid	Hyoid solid	Soft tissue solid	Airway fluid	Interface shell
Node	31153	31223	1735	369933	66498	18720
Element	35271	36548	1924	465847	15927	9388

Table 2 Material properties for FEM model

	Young's modulus (Pa)	Poisson ratio	Density (g mm^{-3})
Bone (skull neck hyoid)	1.37×10^{10}	0.3	1.85×10^{-3}
Soft tissue	1.0×10^4	0.45	1.06×10^{-3}
Nasopharynx	1.37×10^{10}	0.3	1.85×10^{-3}
Thyroid cartilage	2.02×10^6	0.3	1.25×10^{-3}
Cricoid cartilage	2.02×10^6	0.3	1.25×10^{-3}
Epiglottis cartilages	2.02×10^6	0.3	1.25×10^{-3}
Tracheal cartilage	2.02×10^6	0.3	1.25×10^{-3}

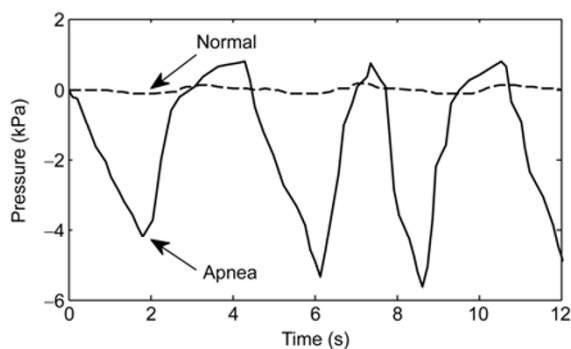


Figure 2 A typical pressure curve in normal and abnormal respiration used in this study.

processes was carried out using a FE software (Adina 8.6, USA), which offers a one-system program that specializes in fluid structure interaction. The main principle of the coupled algorithm in Adina is that the displacement compatibility and the pressure equilibrium along the structure-fluid interfaces should be satisfied. The computation was accomplished with a PC (CPU 3.00 GHz, 8.00 GB RAM) in 12 and 26 h, for the normal episode and apnea episode, respectively.

2 Results

The simulations were conducted with the FSI and CFD methods. A rigid wall condition was used in the CFD case. The flux curves obtained by integrating the velocity on the cross section located on the oropharynx part are illustrated in Figure 3. For a positive value, which corresponds to the expiratory phase, the flux is almost coincident. However, regarding the negative fluxes induced by the negative pressure during the inspiratory phase, the value from the FSI method is obviously smaller than that from the CFD method, particularly around the negative peak value. It is reasonable because based on the FSI method, the large negative pressure caused the cross section to contract severely along the anterior-posterior direction: as a consequence, the area of the cross section reduced about two thirds and the airflow reduced about one third. The smaller the section area is, the less the flux will be. As for the CFD method, there was no area change of the cross section under the rigid wall condition. On the contrary, the cross section increased only a little during the expiratory phase in the FSI simulation. As a result, the corresponding positive fluxes were nearly equal no matter which method was used.

The pressure distribution on the same cross section is illustrated in Figure 4. It can be seen that during the expiratory phase the pressure distribution is generally the same because the structural deformation is very small. The minimum pressure region locates along the anterior wall while the maximum pressure region locates near the posterior wall. Pressure increases from the anterior to the posterior wall in a striped form. As for the inspiratory phase, the minimum

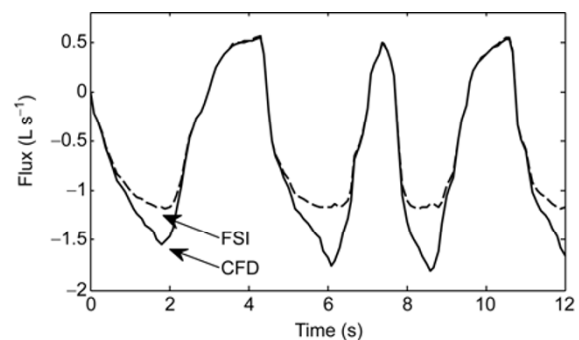


Figure 3 Airflow flux varies as time through a cross section during an apnea episode.

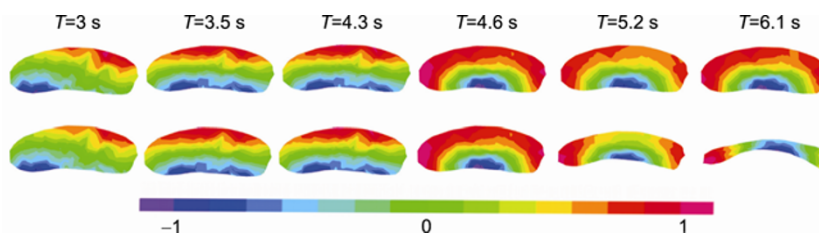


Figure 4 Pressure distribution contour during an apnea episode. The six distributions on the top row were obtained with the CFD method while the six distributions on the bottom row were obtained with the FSI method. $T=3$, 3.5 and 4.3 s belong to the expiratory phase and $T=4.6$, 5.2 and 6.1 s belong to the inspiratory phase.

pressure region focuses on the center of the anterior wall which part is prone to collapse towards the posterior wall. With the FSI method, it can be found that the maximum pressure region locates at both sides of the cross section. This pressure distribution is highly correlated to the collapse mode. At the beginning, the anterior wall undergoes only a tiny displacement towards the posterior wall when the negative pressure value is small. Once this inward displacement occurs, the passageway of airflow will change from an approximately straight shape to a curving shape. As a result, a centripetal force is needed to help the airflow accomplish the curvilinear motion. The pressure gradient pointing from the posterior to the anterior direction gives impetus to this curvilinear motion. On the other hand, the pressure outside of the anterior airway wall stemming from other tissue's gravity and the atmospheric pressure does not change. Thus, the pressure gradient towards the lumen inside increases the deformation of the anterior airway wall. This increased deformation raises the curvature of the airway wall further so that a larger centripetal force is necessary to ensure that the airflow passes the distorted site successfully. In return, this enhanced centripetal force can only be provided by a larger pressure difference. In other words, once an initial displacement inwards occurs, the anterior wall will be easier to collapse if there is no other control function to hold it back. The FSI method can better reveal this positive feedback mechanism between the deformation and the pressure gradient because it takes the structural deformation into account, while the CFD method only focuses on the airflow field. If this positive feedback mechanism is true, then the larger the deformation of the anterior airway wall is, the larger the pressure difference is. This conclusion can be proven and demonstrated by reference to Figure 5. It is easy to observe that the maximum displacement appears at the maximum pressure difference. In other words, the relative anterior-posterior displacement keeps step with the change of the pressure difference. As for the curve from the CFD method, the change of pressure difference is much smaller than with FSI and the correlation between deformation and the pressure difference is not so obvious.

Since the FSI method is superior to the CFD method, it makes sense to carry out a comparison between an apnea breath episode and normal episode only with the FSI method. To show the deformation clearly, a cross section at the

oropharynx was selected and the deformational configurations at typical moments during an apnea episode are illustrated in Figure 6. There is hardly any deformation during the normal episode even when the pressure reaches the peak value. Conversely, it can be seen that the anterior part of the airway wall collapses towards to the posterior part under the large negative pressure. This block obviously reduces the cross section area at the pharynx and as a consequence, the airflow is restricted. Once the airflow decreases to the extent that it is too weak to maintain the normal gas exchange in lung, the apnea episode occurs. It can be found that the displacement of the posterior wall is smaller than the anterior wall because the posterior part of the upper airway is closer to the cervical vertebra, which restrains the defor-

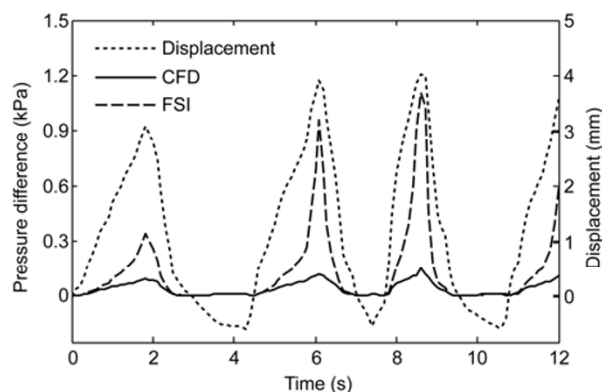


Figure 5 The sagittal displacement history and the pressure difference during an apnea episode obtained from a node on the anterior wall of the oropharynx with the FSI and the CFD methods.

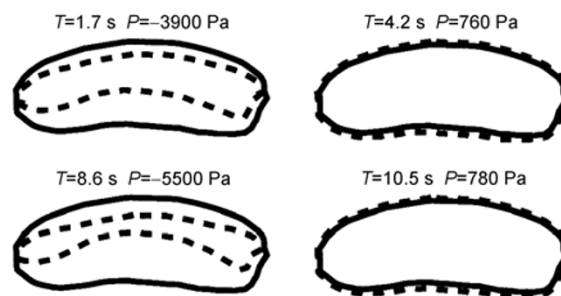


Figure 6 Pressure curve exerted on the outlet during normal breathing and an apnea episode. Four cross sections of the upper airway are extracted at the same location.

mation of soft tissue.

A sagittal section with the profile of the upper airway was chosen to display the strain distribution around the airway during the apnea episode (Figure 7), which can clearly demonstrate the change of the anterior-posterior diameter. It can be seen that the maximum strain is small enough to keep the airway configuration during the expiratory phase while there is an obvious deformation during the inspiratory phase. The strain concentration appears at the pharyngeal portion regardless of whether it is at the expiration or inspiration. The largest strain concentration appears when the pressure peak value reaches as much as 5220 Pa ($T=6.1$ s). The pharyngeal part is a special position where soft tissue is intricate because of the multiple physiological functions. It is at the back region of the soft palate, which is similar to a flexible cantilever beam. In addition, on the other side of the pharyngeal part is the tongue which is a thick layer soft tissue without hard tissue support. It is no wonder that the strain concentration focuses on the pharyngeal part and spreads in a fan-shaped form from the airway wall to the anterior tongue. There is hardly any deformation around the epiglottis because of the support from the thyroid cartilage, cricoids cartilage, epiglottic cartilage and arytenoids cartilage.

3 Discussion

The 3D FE model in this study reconstructs more anatomical details of the upper airway than previous studies. Bony tissues that are adjacent to the upper airway, including the

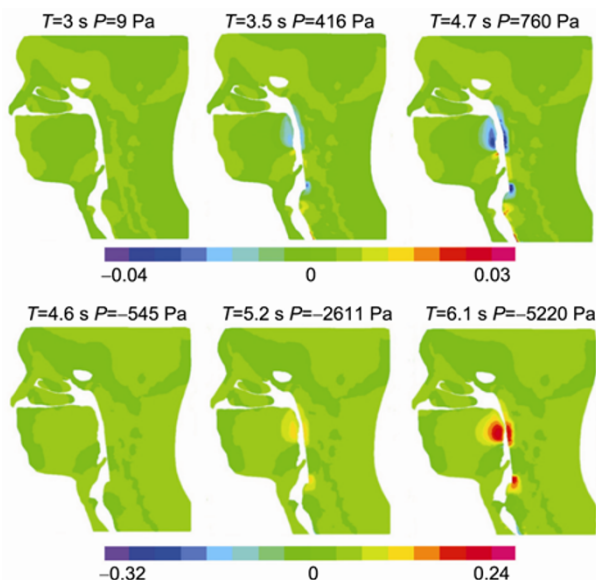


Figure 7 Distribution contours of the strain component along the sagittal direction for the soft tissue around the airway. The strain contour distribution is recorded at the same cross section under the same contour color interval at three different moments with ascending order. The blank space represents the bony tissue and the inside of the upper airway.

skull, cervical vertebra, thyroid cartilage, cricoids cartilage, epiglottis cartilage, and tracheal cartilage as well as the surrounding soft tissue are embodied. It is worth emphasizing that the diversity of mechanical properties for the upper airway is taken into account by using a layer of shell elements to consider the different influences of bony tissues. This FE model not only makes it possible to reach a more accurate airflow simulation but also can reflect the important role of supporting tissues during breathing by using the FSI method.

Up to now, similar works with the FSI method [19–23] have usually focused on the local structure's influence on airflow inside the upper airway. In contrast to these studies, the whole upper airway as well as the surrounding tissues was considered in the FSI simulation presented in this paper. More importantly, the results reveal a positive feedback mechanism for the collapse of the upper airway during the apnea episode. Under a large negative pressure, the deformation of the anterior airway wall and the pressure gradient on the cross section strengthen each other and lead to upper airway collapse and apnea. Thus it can be concluded that the initial configuration of the upper airway, especially the original curvature of the anterior airway wall, is closely correlated to OSAS. This can explain why those persons whose upper airways are too curving or narrow for some reasons, such as when body fat accumulates around the neck, are prone to be vulnerable with sleep apnea. This conclusion can also offer a theoretical basis for clinical treatment with MMA (maxilla-mandibular advancement), which improves the initial configuration of the upper airway [25,26].

As has been discussed, the weak or absence of nerve control mechanism is one of the important factors for OSAS. For most people, even though the configuration of the upper airway may be naturally concave inward to a certain extent, the normal nerve control mechanism helps to weaken or eliminate the positive feedback. As a result, the airway can still be kept unobstructed and breathing can be kept normal without apnea. The nerve control functions as a feedback mechanism. However, for some OSAS patients, once the deformation of the airway wall reaches a certain level, the collapse becomes an inevitable consequence due to a deficiency of negative feedback control from the surrounding muscles. To date, there has been little study of nerve control mechanisms in respiration.

The load condition in the inlet and outlet is very important because the airflow in the upper airway during normal breathing or an apnea episode is driven by the pressure variation. By now, it is accustomed to assign an idealized flux in the inlet and a velocity or pressure in the outlet, since it is easy to measure the velocity and pressure variation in the inlet while they are difficult to obtain inside the deeper part of the upper airway. Most of the previous studies assume the airflow velocity or pressure as a regular periodic triangle waveform or sinusoidal waveform whose

peak value depends on the tidal volume [19–23]. Yet there exists a shortage for this type of load condition which makes the total flux during the whole breath simulation to be a constant. For some cases, the airway does not need to completely close when the apnea occurs. A large collapse can obviously reduce the flux and also led to apnea. This is called OSAHS (obstructive sleep apnea hypopnea syndrome) which is one subtype of OSAS. If the whole flux is restricted to a constant value, then this kind of OSAS cannot be simulated correctly. In this study, both the inlet and outlet exerted a pressure variable which was measured inside the upper airway [24]. Under this type of load condition, the whole flux is variable according to the actual flow condition. This can be explicitly demonstrated by the diagram given in Figure 3. There is a distinct difference between the flux-time curve obtained with the CFD and FSI methods, respectively, during the large negative pressure duration when the airway wall deforms intensely and therefore, the airflow is restricted at the blocked site.

The location where the collapse most likely happens is a major research interest. It is important to pay more attention to the soft tissue which tends to deform as well as the velopharynx and oropharynx where the obstruction is often observed in OSAS patients. The base of the tongue and the posterior of the soft palate are most prone to collapse. The results of this simulation are consistent with clinical observations. It does not matter if it is during the inspiration or expiration phase, the strain concentration lies on the root of tongue, which can be seen in Figure 4. This is reasonable because this domain is far from hard tissue and corresponds to the narrowest section of the upper airway, where large negative pressure may occur because of the faster flow velocity. The upper end of this segment is connected to the nasal cavity while the other is connected to the epiglottis region. The former is connected to the hard palate and the latter is surrounded by a group of cartilage, such as the thyroid cartilage and epiglottis cartilage. Only the middle part, namely the root of the tongue, has a lower elastic modulus compared to both ends. It is just like a flexible tube with two ends fixed. It is thus apparent that this part is prone to collapse.

4 Conclusion

In this study, a finite element model including the airway, skull, neck, hyoid and soft tissue around the upper airway was developed. Both CFD and FSI simulations were performed for normal breathing and an apnea episode. FSI simulation can supply a more realistic result than CFD. The simulation results show a positive feedback mechanism of the upper airway collapse during apnea, which supplies meaningful information for clinical treatment and further research of OSAS.

This work was supported by the Beijing Natural Science Foundation (3122020).

- 1 Lan Z, Itoi A, Takashima M, et al. Difference of pharyngeal morphology and mechanical property between OSAHS patients and normal subjects. *Auris Nasus Larynx* 2006, 33: 433–439
- 2 Ryan C M, Bradley T D. Pathogenesis of obstructive sleep apnea. *J Appl Physiol*, 2005, 99: 2440–2450
- 3 White D P. Pathogenesis of obstructive and central sleep apnea. *Am J Respir Crit Care Med*, 2005, 172: 1363–1370
- 4 Steier J, Jolley C J, Seymour J, et al. Increased load on the respiratory muscles in obstructive sleep apnea. *Respir Physiol Neurobiol*, 2010, 171: 54–60
- 5 Horner R L. The neuropharmacology of upper airway motor control in the awake and asleep states: implications for obstructive sleep apnoea. *Respir Res*, 2001, 2: 286–294
- 6 Huang L, Quinn S J, Ellis P D M, et al. Biomechanics of snoring. *Endeavour*, 1995, 19: 96–100
- 7 Farrè R, Rigau J, Montserrat J M, et al. Static and dynamic upper airway obstruction in sleep apnea. *Am J Respir Crit Care Med*, 2003, 168: 659–663
- 8 Luo X Y, Pedley T J. Multiple solutions and flow limitation in collapsible channel flows. *J Fluid Mech*, 2000, 420: 301–324
- 9 Huang L, Williams J E F. Neuromechanical interaction in human snoring and upper airway obstruction. *J Appl Physiol*, 1999, 86: 1759–1763
- 10 Fodil R, Ribreau C, Louis B. Interaction between steady flow and individualized compliant segment: application to upper airways. *Med Biol Eng Comput*, 1997, 35: 638–648
- 11 Lazopoulos K, Lazopoulos K A, Palassopoulos G. On the stability of the upper airways system. *Nonlinear Analysis. Real World Appl*, 2011, 12: 1323–1337
- 12 Saksono P H, Nithiarasu P, Sazonov I, et al. Computational flow studies in a subject-specific human upper airway using a one-equation turbulence model. Influence of the nasal cavity. *Int J Numer Meth Eng*, 2011, 87: 96–114
- 13 Sittitavornwong S, Waite P D, Shih A M, et al. Evaluation of obstructive sleep apnea syndrome by computational fluid dynamics. *Sem Orthod*, 2009, 15: 105–131
- 14 Mylavarapu G, Murugappan S, Mihaescu M, et al. Validation of computational fluid dynamics methodology used for human upper airway flow simulations. *J Biomech*, 2009, 42: 1553–1559
- 15 Mihaescu M, Murugappan S. Large Eddy simulation and Reynolds-averaged Navier-Stokes modeling of flow in a realistic pharyngeal airway model: an investigation of obstructive sleep apnea. *J Biomech*, 2008, 41: 2279–2288
- 16 Zhang J, Liu Y, Sun X. Computational fluid dynamics simulations of respiratory airflow in human nasal cavity and its characteristic dimension study. *Acta Mech Sin*, 2008, 24: 223–228
- 17 Liu Y, Yu C, Sun X, et al. 3D FE model reconstruction and numerical simulation of airflow for the upper airway. *World J Model Simul*, 2006, 2: 190–195
- 18 Xu C, Sin S H, McDonough J M, et al. Computational fluid dynamics modeling of the upper airway of children with obstructive sleep apnea syndrome in steady flow. *J Biomech*, 2006, 39: 2043–2054
- 19 Malvè M, del Palomar A P, López-Villalobos J L, et al. FSI analysis of the coughing mechanism in a human trachea. *Ann Biomed Eng*, 2010, 38: 1556–1565
- 20 Xu C, Brennick M J, Dougherty L. Modeling upper airway collapse by a finite element model with regional tissue properties. *Med Eng Phys*, 2009, 31: 1343–1348
- 21 Chouly F, Van Hirtum A, Lagrée P Y, et al. Numerical and experimental study of expiratory flow in the case of major upper airway obstructions with fluid-structure interaction. *J Fluids Struct*, 2008, 24: 250–269
- 22 Sun X, Yu C, Wang Y, et al. Numerical simulation of soft palate movement and airflow in human upper airway by fluid-structure interaction method. *Acta Mech Sin*, 2007, 23: 359–367

- 23 Payan Y, Pelorson X. Physical modeling of airflow-walls interactions to understand the sleep apnea syndrome. *Lect Note Comput Sci*, 2003, 2673: 261–269
- 24 Liu Y, Bao Y, Liu W, et al. An analysis of pharyngeal respiratory pressure before and after onset of obstruction in respiratory obstructive sleep apnea hypopnea syndrome. *Chin J Intern Med*, 2006, 45: 914–917
- 25 Ronchi P, Novelli G, Colombo L S, et al. Effectiveness of maxilla-mandibular advancement in obstructive sleep apnea patients with and without skeletal anomalies. *Int J Oral Maxil Surg*, 2010, 39: 541–547
- 26 Holty J E C, Guilleminault C. Maxillomandibular advancement for the treatment of obstructive sleep apnea: a systematic review and meta-analysis. *Sleep Med Rev*, 2010, 14: 287–297

Open Access This article is distributed under the terms of the Creative Commons Attribution License which permits any use, distribution, and reproduction in any medium, provided the original author(s) and source are credited.